

UC San Diego

UC San Diego Previously Published Works

Title

Exploiting the receptor-binding domains of RSPO1 to target LGR5-expressing stem cells in ovarian cancer

Permalink

<https://escholarship.org/uc/item/5cz7v9xm>

Journal

Journal of Pharmacology and Experimental Therapeutics, 385(2)

ISSN

0022-3565

Authors

Wong, Clara

Mulero, Maria Carmen

Barth, Erika I

et al.

Publication Date


2023-05-01

DOI

10.1124/jpet.122.001495

Peer reviewed

Exploiting the Receptor-Binding Domains of R-Spondin 1 to Target Leucine-Rich Repeat-Containing G-Coupled Protein Receptor 5-Expressing Stem Cells in Ovarian Cancer[□]

Clara Wong,¹ Maria Carmen Mulero,¹ Erika I. Barth, Katherine Wang, Xiyang Shang, Sanika Tikle,² Catherine Rice, Dennis Gately, and  Stephen B. Howell

Moore's Cancer Center and Department of Medicine, University of California, San Diego, 3855 Health Sciences Drive, Mail Code 0819, La Jolla, California

Received November 2, 2022; accepted February 8, 2023

ABSTRACT

Leucine-rich repeat-containing G-protein-coupled receptor (LGR5) and LGR6 mark epithelial stem cells in normal tissues and tumors. They are expressed by stem cells in the ovarian surface and fallopian tube epithelia from which ovarian cancer arises. High-grade serous ovarian cancer is unique in expressing unusually high levels of LGR5 and LGR6 mRNA. R-spondins are the natural ligands for LGR5 and LGR6 to which they bind with nanomolar affinity. To target stem cells in ovarian cancer, we used the sortase reaction to site-specifically conjugate the potent cytotoxin monomethyl auristatin E (MMAE) via a protease sensitive linker to the two furin-like domains of RSPO1 (Fu₁-Fu₂) that mediate its binding to LGR5 and LGR6 and their co-receptors Zinc And Ring Finger 3 and Ring Finger Protein 43 via a protease-cleavable linker. An immunoglobulin Fc domain added to the N-terminal end served to dimerize the receptor-binding domains so that each molecule carries two MMAE. The resulting molecule, FcF2-MMAE, demonstrated: 1) selective LGR5-dependent low nanomolar cytotoxicity against ovarian cancer cells *in vitro*; 2) selectivity that was dependent on binding to

both the LGR receptors and ubiquitin ligase co-receptors; 3) favorable stability and plasma pharmacokinetic properties when administered intravenously with an elimination half-life of 29.7 hours; 4) selective inhibition of LGR5-rich as opposed to isogenic LGR5-poor tumors *in vivo*; and, 5) therapeutic efficacy in three aggressive wild-type human ovarian cancer xenograft models. These results demonstrate the successful use of the Fu₁-Fu₂ domain of RSPO1 as a drug carrier and the ability of FcF2-MMAE to target cells in tumors that express stem cell markers.

SIGNIFICANCE STATEMENT

FcF2-MMAE is a novel cancer therapeutic that exploits the high-affinity binding domains of RSPO1 to target monomethyl auristatin E to tumor stem cells that express LGR5. FcF2-MMAE has low nanomolar LGR5-dependent cytotoxicity *in vitro*, favorable pharmacokinetics, and differential efficacy in an isogenic LGR5-poor versus LGR5-rich ovarian cancer xenograft model when given on a weekly schedule.

Introduction

The small population of stem cells that sustain epithelia throughout the body proliferate and subsequently differentiate in response to growth factors in their niche and their progeny progress through a series of transcriptional states as they differentiate and lose proliferative potential (Clarke, 2019). Signaling in the wingless integration site protein (WNT)

pathways control fate decisions during embryogenesis and in many adult tissues (Raslan and Yoon, 2019). WNT signaling is regulated by a combination of WNT ligands that bind to various kinds of frizzled receptors, and R-spondins (RSPOs) that bind to leucine-rich repeat-containing G protein-coupled receptors (LGRs). Cells in the immediate environment of the stem cell niche are the major source of the ligands that drive the WNT signaling and the most effective signaling molecules appear to be transmitted to stem cells over very short distances. RSPO1 has a dominant but not exclusive position among the 4 members of the RSPO family in malignant tissues, and among the members of the LGR family of receptors, most evidence points toward LGR5 and LGR6 as having pivotal roles (Yan et al., 2017).

Solid tumors have cell subpopulations that exhibit many of the characteristics of stem cells, such as the ability to form spheroids or initiate new tumors. As for stem cells residing in

This research was supported by the Clayton Medical Research Foundation and the National Institutes of Health National Cancer Institute [Grant CA023100]. The authors express their appreciation to Dr. Karl Willert for advice and the HEK293 STF cells.

The authors declare no conflicts of interest.

¹C.W. and M.C.M. contributed equally to this work.

²Current affiliation: InterVenn Biosciences, South San Francisco, California.

dx.doi.org/10.1124/jpet.122.001495.

[□] This article has supplemental material available at jpet.aspetjournals.org.

ABBREVIATIONS: ADC, antibody-drug conjugate; CSC, cancer stem cells; Fu₁-Fu₂, the first and second furin domains of RSPO1; HPLC, high-pressure liquid chromatography; LGR, leucine-rich repeat-containing G-protein-coupled receptor; LLQ, lower limit of quantitation; MMAE, monomethylauristatin E; Ni-NTA, nickel nitrilotriacetic acid; RNF43, Ring Finger Protein 43; RSPO, R-spondin; STF, Super Topflash; WNT, wingless integration site protein; ZNRF3, Zinc And Ring Finger 3.

organized epithelia, many cancer stem cells (CSCs) require an RSPO to grow vigorously when cultured (Sato et al., 2009; Barker et al., 2010). Elimination of the small fraction of cells in a tumor that are CSCs should eventually stop further tumor expansion by reducing the supply of the more differentiated cells that make up the bulk of the population. Recent studies have disclosed a level of plasticity that may allow some cells that have moved out of the transcriptional state of the CSCs to revert (Gupta et al., 2019), but finding ways of killing CSCs remains a major therapeutic goal.

High-grade serous ovarian cancer can arise from either the ovarian surface epithelium or the epithelium of the fallopian tube, although the latter predominates (Zhang et al., 2019). Lineage tracing studies in mice suggest that LGR5 marks a stem cell population in the ovary, and LGR6 marks stem cells in the mouse and human fallopian tube epithelium (de Lau et al., 2014; Kessler et al., 2015; Zhang et al., 2019). Review of data from The Cancer Genome Atlas disclosed that high grade serous ovarian cancer expresses high levels of LGR5 and LGR6 mRNA. In addition, with the exception of mesothelioma, ovarian cancer has the highest median expression of RSPO1 mRNA when compared with all other tumor types in the database (Schindler et al., 2017). This suggested that ovarian cancers rely on RSPO1 to support their CSC population and that they are well equipped to bind and internalize it. Our hypothesis was that we could take advantage of this dependency by systemically administering the receptor binding domain of RSPO1 armed with a cytotoxin.

We report here on studies showing that the Fu₁-Fu₂ receptor-binding domain of RSPO1 can be used to target monomethyl auristatin E (MMAE) to ovarian cancer cells rich in stem cell receptor LGR5. A modified IgG1 Fc domain containing half-life extending modifications (Lee et al., 2019) was linked to the N-terminal end of the Fu₁-Fu₂ domain which bore a sortase recognition sequence on its C-terminal end. During synthesis of this protein in HEK293E cells, the 2 chains are linked by intermolecular disulfide bonds between the Fc domains, resulting in a dimeric molecule capable of being conjugated with 2 MMAE molecules using the sortase reaction to create FcF2-MMAE (Fig. 1). This molecule displays low nM cytotoxicity in a panel of human ovarian cancer cell lines and has a favorable stability and pharmacokinetic profile.

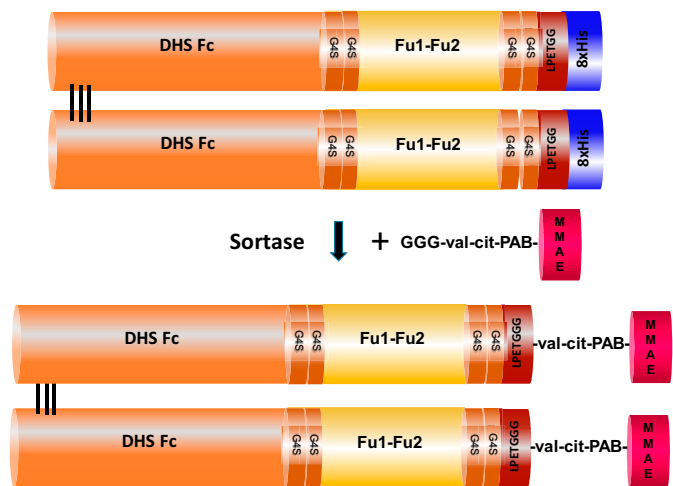


Fig. 1. Schematic diagram of FcF2-His and its conversion to FcF2-MMAE using the sortase reaction.

Moreover, FcF2-MMAE produces selective killing of LGR5-rich tumor cells *in vitro* and differential inhibition of the growth of isogenic LGR5-poor and LGR5-rich tumors *in vivo*. It exhibits activity in three wild-type human ovarian cancer xenograft models on a clinically relevant dose schedule, and at doses that produce only transient adverse events. Although our work has focused on ovarian cancer, given that stem cells of many other tumor types also express LGR5/LGR6, there is the possibility that FcF2-MMAE can limit the growth of additional types of cancer. FcF2-MMAE expands on the concept of arming an endogenous ligand of a stem cell-specific receptor to create a novel cancer therapeutic.

Materials and Methods

Reagents and Cell Lines. Antibodies were from the following sources: anti-RSPO1, clone OTI1A9, OriGene, Inc; anti-MMAE, clone B11F11, Levena Biopharma; hLGR5/GPR49 antibody Cat# MAB8078, R&D Systems; PE-conjugated anti-mouse IgG antibody Cat# F0102B, R&D Systems. Nickel nitrilotriacetic acid (Ni-NTA) resin was purchased from Qiagen, and SP-sepharose and DEAE resins from GE Healthcare Life Sciences. Propidium iodide was purchased from ThermoFisher (Cat# P3566). All ovarian cancer cell lines were acquired either from the American Type Culture Collection or from laboratories in the United States; all cell lines were STR verified at the American Type Culture Collection. The HEK293 STF cells were provided by Dr. Karl Willert, University of California, San Diego. The sortase plasmid vector pet30b-7M SrtA was purchased from Addgene. Sortase-6xHis containing mutations P94R, E105K, E108Q, D160N, D165A, K190E, and K196T was produced in *Escherichia coli* strain Rosetta and purified using Ni-NTA resin chromatography as previously described (Yu et al., 2021). (Gly)₃-vc-PAB-MMAE was synthesized by Levena Biopharma. Plasma levels of FcF2-MMAE were determined using an ELISA kit from R&D Systems (DY4645-05).

Synthesis and Purification of FcF2-His. FcF2-His was produced by transient transfection of a pcDNA3.1 vector containing an insert coding for the IgG Fc domain linked to Fu₁-Fu₂ domain of RSPO1 into HEK293E cells. Cells were grown in 5% CO₂ at 37°C in 300 mL of HEK293E Culture Media, which consists of 150 mL Gibco FreeStyle 293 Medium (Cat# 12338-026, ThermoFisher), 150 mL HyClone SFM4HEK293 media (Cat# 82003-356), 6 mL Fetal Bovine Serum (Cat# 26140-079, ThermoFisher), 333 uL G418 Sulfate (Cat# G8168, Sigma), and 333 μL of anti-clumping agent (Cat# 0010057AE, ThermoFisher) in 1 L flasks on a platform rotating at 130 rpm. Cell supernates were harvested after 5 days of culture, centrifuged to sediment debris and then loaded onto a column containing Ni-NTA resin (Cat# 30250, Qiagen) that was equilibrated with buffer containing 150 mM NaCl, 20 mM Tris, pH 7.6. After washing, the FcF2-His protein was eluted with buffer containing 300 mM imidazole, 150 mM NaCl, 20 mM Tris, pH 7.6. The eluates were diluted 1:3 with 20 mM Tris, pH 7.6 and then loaded on a DEAE column. The concentration of the flow through from the DEAE column was quantified by reverse-phase high-pressure liquid chromatography (HPLC) analysis using a C4 column.

Conjugation of FcF2-His to MMAE using Sortase. The sortase enzyme recognizes and forms a transient intermediate with the threonine in the amino acid sequence LPETGG in the C-terminal section of FcF2-His. The sortase is then displaced by the (Gly)₃-val/cit-PAB-MMAE linker with the resultant formation of a new peptide bond between the FcF2-LPETGG and the linker. The sortase reaction was carried out for 4 hours at 37°C with the FcF2-His immobilized on SP-sepharose resin (Cat# 17072901, Cytiva); the reaction mixture contained (Gly)₃-vc-PAB-MMAE and FcF2-His at a molar ratio of 20:1, and sortase-6xHis and FcF2-His at a molar ratio of 1:4. After washing the SP-sepharose to remove the sortase-6xHis and unreacted (Gly)₃-vc-PAB-MMAE, the purified FcF2-MMAE was eluted with phosphate

buffer containing 1 M NaCl, pH 8.0. FcF2-MMAE was diluted to a NaCl concentration of 200 mM before being sterilized with a 0.22 μm filter and stored frozen at -80°C .

Flow Cytometric Analysis. Expression of LGR5 in live cells was determined by flow cytometry after staining with anti-hLGR5/GPR49 antibody at a final concentration of 12.5 $\mu\text{g}/\text{mL}$ for 30 minutes at 25°C protected from light. Excess anti-hLGR5/GPR49 antibody was removed with two rounds of PBS wash, and the cells were incubated with PE-conjugated anti-mouse IgG antibody diluted 1:20 for 30 minutes at 25°C protected from light. Excess anti-mouse IgG antibody was removed with two rounds of PBS wash, and the cells were resuspended in 300 μL of PBS with 0.5 $\mu\text{g}/\text{mL}$ of propidium iodide. The prepared cell suspension was analyzed on a BD FACSAria II flow cytometer.

Growth Rate Inhibition Assay. The effect of FcF2-MMAE on cell growth rate in vitro was determined using the CCK8 reagent (Dojindo, Inc). Cells were seeded in triplicate wells for each drug concentration at densities sufficient for control wells to yield an OD450 of >1.5 after subtraction of the OD determined at the time drug exposure was started. Survival was calculated as percent reduction of the difference in the $T = 0$ and the time the assay was stopped (Hafner et al., 2016). All data points represent the mean \pm S.E.M. of triplicate cultures for each concentration of the tested drug.

Super TopFlash (STF) Assay. STF cells were seeded at 50,000 cells/well in 0.3 mL of Dulbecco's modified Eagle's medium containing 10% fetal bovine serum and 1% penicillin/streptomycin in a white 96-well plate and grown overnight. The medium was replaced with the sample to be tested and WNT conditioned medium at a final dilution of 1:6. After a 20-hour incubation, the medium was removed, and cells were lysed with 20 μL of 1X cell lysis buffer (Promega). Luminescence was recorded immediately after addition of 100 μL of Luciferase Reagent using a Tecan plate reader.

Pharmacokinetic Studies. BALB/c female 8-week-old mice were injected intravenously with FcF2-MMAE at a dose of 0.1 nmol/g and blood was collected in EDTA-coated tubes from the cheek or tail vein at timed intervals. Plasma FcF2-MMAE concentration was determined by ELISA using capture and detection antibodies specific for human RSPO1 that recognize the Fu₁ and Fu₂ subdomains. Pharmacokinetic parameters were assessed using Phoenix WinNonlin version 8.1 (Certara Inc., Princeton, NJ, USA).

Efficacy Studies. BALB/c female 6- to 8-week-old nu/nu mice were obtained from the UCSD breeding colony and inoculated subcutaneously with tumor cells harvested from culture and mixed 2:1 vol/vol with Matrigel prior to injection of 150 μL of the mixture. The number of cells inoculated varied with the tumor type: OVCAR8/EV and OVCAR8/LGR5, $2.5 \times 10^6/\text{site}$; KF-28, $2.5 \times 10^6/\text{site}$; CAOv3, $5 \times 10^6/\text{site}$. Tumor growth rate was determined from measurements of the crossed diameters measured once or twice a week using the formula $V = (w^2 \times L)/2$. Control mice received vehicle alone (phosphate buffered saline with 0.02% Tween-20) on the same schedule.

Data Presentation. All data are presented as mean \pm S.E.M. of two or more independent experiments each performed with triplicate cultures.

Results

Design of FcF2-His. The upper portion of Fig. 1 presents a schematic diagram of FcF2-His. The protein contains a variant human IgG1 Fc domain (Lee et al., 2019) connected through two Gly₄Ser spacers to the Fu₁-Fu₂ domains of human RSPO1. Two further Gly₄Ser spacers separate the Fu₁-Fu₂ domains from the LPETGG sortase recognition sequence which is followed by an 8xHis tag that facilitates purification. Each Fc-(Fu₁-Fu₂)-LPETGG-His (abbreviated FcF2-His) sequence contains 391 amino acids. The Fc domain causes dimerization via three intermolecular disulfide bonds, the bond that links the Fc to the light chain in an antibody and the two bonds that

link the Fc domains together at their hinge region. The resulting protein has an overall calculated MW of 85,284 Da. Glycosylation is present on the Fc domain and on residue N137 in the Fu₁-Fu₂ domain (RSPO1 numbering).

Sortase-Mediated Conjugation of Monomethyl Auristatin E (MMAE). The lower portion of Fig. 1 shows a schematic of the conversion of FcF2-His to FcF2-MMAE. The sortase enzyme cleaves the LPETGG sequence between the threonine and glycine and forms a transient thioester bond with a cysteine in the active site of the enzyme, which is subsequently attacked by the N-terminal glycine of the protease sensitive GGG-vc-PAB-MMAE linker. The His tag is lost in the reaction. This results in the precise covalent loading of one molecule of MMAE on each arm of the FcF2-His and the production of a homogeneous population of conjugated FcF2-MMAE molecules.

FcF2-MMAE Production, Purification, and Characterization. FcF2-His was produced by transient transfection of the vector pcDNA3.1-FcF2-8xHis into HEK293E cells and purified from cell supernates by capture on Ni-NTA resin and subsequent ion exchange chromatography. The FcF2-His was then reacted with sortase-His and GGG-vc-PAB-MMAE for 4 hours at 37°C to produce FcF2-MMAE. Across 14 batches, the average yield of FcF2-His was 23.4 ± 2.3 mg/L, sortase efficiency was $77 \pm 8.6\%$, and the yield of final product was 18.8 ± 3.5 mg/L (mean \pm S.E.M.).

Fig. 2 shows the results of characterization of FcF2-His and FcF2-MMAE by reverse-phase HPLC, size exclusion chromatography, and reducing and non-reducing SDS-PAGE. On reverse-phase HPLC analysis using a C4 column both forms of the molecule run as a single well-defined peak (Fig. 2, A and D). Analysis on an HPLC 300 size-exclusion column indicated that FcF2-His and FcF2-MMAE exist in solution both as a dimer, and a dimer of the already dimeric molecule (Fig. 2, B and E), hereafter referred to as the tetramer. A small amount of higher MW species (7%) eluted just before the major tetramer peak of FcF2-His; FcF2-MMAE contains a third lower MW peak. The non-reducing SDS-PAGE analysis of FcF2-His (Fig. 2C) showed that, in the presence of SDS detergent in the loading buffer, most of the tetramer runs at a MW consistent with the size of the FcF2-His dimer (85.3 kD). Under reducing conditions, the bulk of the protein runs as a doublet at ~ 42 – 46 kD. To refine understanding of this doublet, the FcF2-His was treated with PNGase to remove the N-linked sugars. As shown in Supplemental Fig. 1A, this resulted in the collapse of the doublet to a single band consistent with the conclusion that the doublet is attributable to differential glycosylation. When the single glycosylation site in the Fu₂ domain at N137 was mutated to an alanine, the doublet was lost. Extensive comparison of the wild-type and N137A forms of a molecule containing just the Fu₁-Fu₂ domains coupled to MMAE demonstrated no change in cytotoxicity or plasma pharmacokinetics indicating that glycosylation at this site had little functional consequence with respect to these parameters.

Non-reducing SDS-PAGE analysis of FcF2-MMAE (Fig. 2E) showed that, in the presence of the SDS detergent in the loading buffer, the bulk of the FcF2-MMAE runs at a MW of 72–78 kD and that, when run under reducing conditions, it runs at 42–48 kD in a manner similar to the behavior of FcF2-His under non-reducing and reducing conditions. Western blot analysis of FcF2-MMAE using anti-RSPO1 and anti-MMAE antibodies indicated that the major bands that stain for

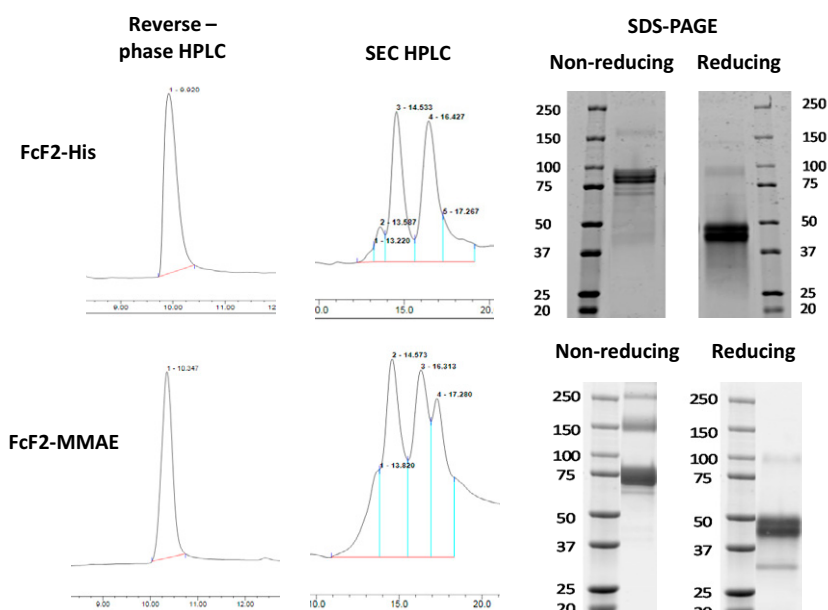


Fig. 2. Analytic characterization of FcF2-His and FcF2-MMAE. A–C, analysis of FcF2-His; D–F, analysis of FcF2-MMAE. A and D, reverse-phase HPLC analysis (C4 column); B and E, HPLC-based size exclusion analysis (SEC300 column). C and F, SDS-PAGE analysis under non-reducing and reducing conditions stained with Instant Blue.

protein on the SDS-PAGE gels contain all components of the molecule (Fc, Fu₁-Fu₂, and MMAE) (Supplemental Fig. 1B) and this was confirmed also for all the major peaks visible in the C4 and SEC300 profiles.

In Vitro Cytotoxicity and Selectivity of FcF2-MMAE. HEK293 cells and the human ovarian carcinoma cell line OVCAR8 were molecularly engineered to stably express increased levels of LGR5. The parental forms of both of these lines express variable but poorly defined levels of all 3 LGR receptors. Flow cytometric analysis using an antibody to LGR5 documented 8.7-fold higher levels of LGR5 in the HEK293/LGR5 cells than in the HEK293/EV controls; in the case of the OVCAR8 cells the difference was ~25-fold (Supplemental Fig. 2, A and B, respectively). Cytotoxicity assays were carried out using a 120-hour exposure to drug and the CCK8 reagent to assess viability. Fig. 3, A and B shows LGR5 receptor-dependent cytotoxicity in the isogenic HEK293 pair; for two batches tested the IC₅₀ values of HEK293/LGR5 cells were 21- and 46-fold more sensitive than the HEK293/EV cells. A large differential effect was also observed when tested using the OVCAR8/EV and OVCAR8/LGR5 isogenic pair; the two recent batches demonstrated a 77- and 87-fold differential IC inhibition of cell growth (Fig. 3, C and D). Across recent batches that met all release criteria, the mean IC₅₀ for the OVCAR8/EV cells was 4.9 ± 1.1 nM (S.E.M.) and for the OVCAR8/LGR5 cells, it was 0.094 ± 0.038 nM; the mean ratio of IC₅₀ values was 65 ± 12.7 ($N = 4$).

The question of whether the differential inhibition of growth of LGR5-poor and LGR5-rich isogenic pairs could be due to differences in sensitivity to free MMAE instead of Fu₁-Fu₂-directed targeting was addressed by using the same assay to determine IC₅₀ values for free MMAE. HEK293/LGR5 cells were 1.6-fold more resistant to free MMAE than the HEK293/EV cells (19.2 ± 0.4 versus 30.5 ± 2.5 , $P = 0.03$ $N = 3$). The OVCAR8/LGR5 cells were 1.5-fold more resistant to free MMAE than the OVCAR8/EV cells (IC₅₀ values 129 versus 85 nM, respectively). Thus, both of the LGR5-rich cell types were actually slightly resistant to free MMAE providing

confidence that the selectivity exhibited by FcF2-MMAE is due to targeting by the Fu₁-Fu₂ domains.

Further evidence was provided by the observation that treatment of a population of OVCAR8 cells with FcF2-MMAE deleted it of LGR5-positive cells. A mixed population of OVCAR8 cells expressing low and higher levels of LGR5 cells were exposed to 10 nM FcF2-MMAE for 96 hours. Prior to treatment flow cytometric analysis demonstrated a bi-modal distribution of LGR5-expressing cells (Supplemental Fig. 2C). FcF2-MMAE treatment caused the loss of a large fraction of the cells expressing high levels of LGR5 but produced substantially less effect on the fraction of cells with low-level LGR5 expression. In addition to differences in IC₅₀ values, this data provides evidence of differential killing as a function of LGR5 expression level.

Cytotoxicity to Human Wild-Type Ovarian Cancer Cell Lines. To assist in the selection of appropriate xenograft models for efficacy testing, the cytotoxicity of FcF2-MMAE was determined for a panel of eight human ovarian carcinoma cell lines. The concentration-survival curves shown in Fig. 3E indicate that the IC₅₀ values ranged from 3.8 to 29.6 nM; the IC₅₀ was < 10 nM in seven of eight cell lines. Thus, although the level of the sum of all LGR expression is not known for these cell lines, the data indicates that FcF2-MMAE is very potent across this panel of ovarian carcinoma cell lines.

Determinants of Cytotoxic Selectivity. RSP01 is a bispecific ligand. The Fu₁ domain of RSP01 binds to the ubiquitin ligase receptors ZNRF3 and RNF43 and the Fu₂ domain binds to LGR4, LGR5, and LGR6. The relative contribution of each of these types of receptors to the selectivity of FcF2-MMAE for the OVCAR8/EV and OVCAR8/LGR5 cells was explored by introducing mutations in one or the other Fu domain that were previously documented to disable binding to its cognate receptor (Peng et al., 2013; Xie et al., 2013; Zebisch et al., 2013; Zhang et al., 2020; Cui et al., 2021). The cytotoxicity of the mutant forms was tested in the in vitro OVCAR8/EV and OVCAR8/LGR5 model. The growth inhibition curves presented in Fig. 4A indicate that both domains contribute importantly to the selectivity of FcF2-MMAE. The Q71R mutation in Fu₁ reduced the IC₅₀ ratio from 19.5 to 5.1 ($P = 0.05$), the

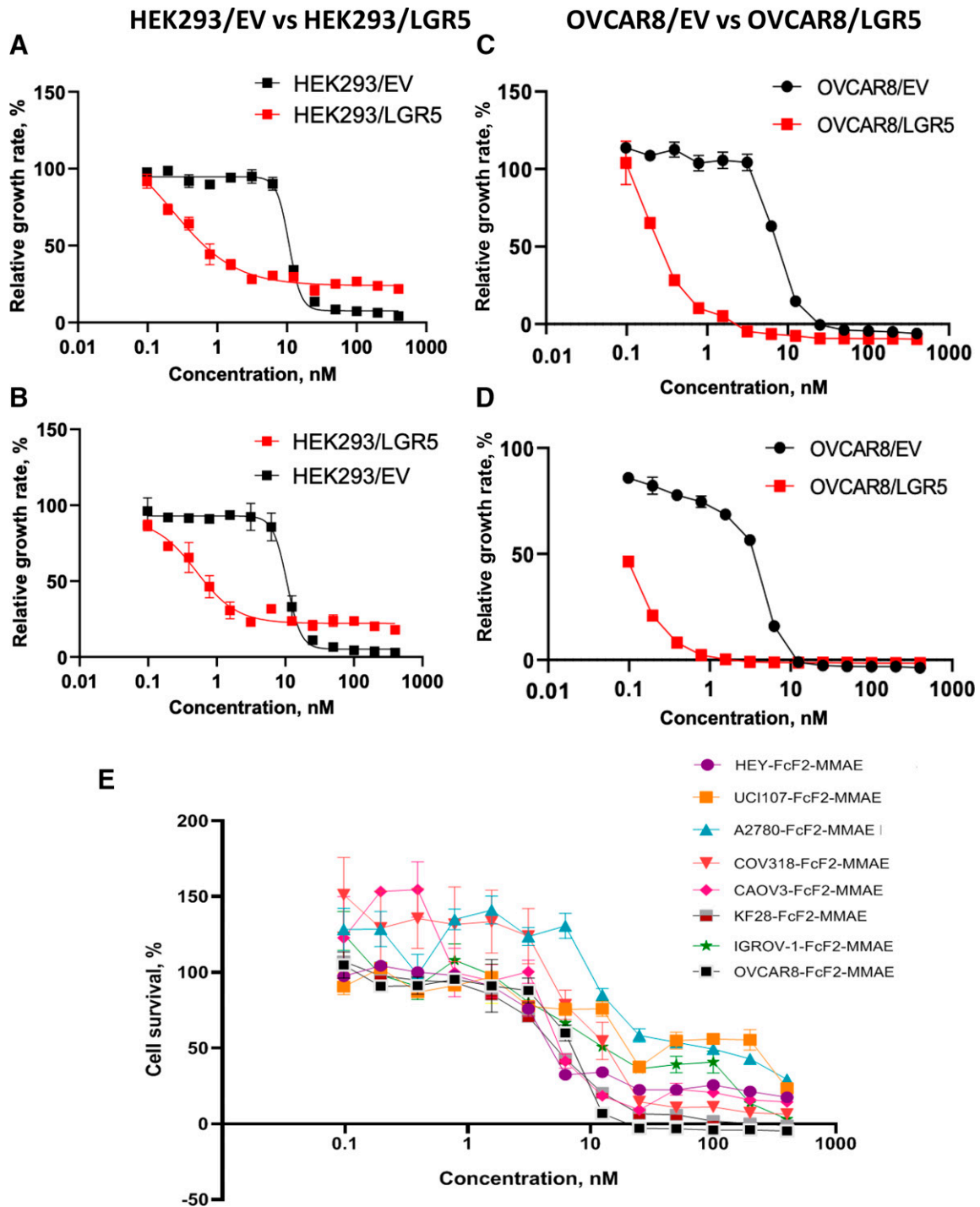


Fig. 3. Cytotoxicity of FcF2-MMAE to cell lines. Potency and selective cytotoxicity of two representative batches of FcF2-MMAE in HEK293/EV versus HEK293/LGR5 (A and B), and two other representative batches in the OVCAR8/EV versus OVCAR8/LGR5 models (C and D). E, Potency of FcF2-MMAE against eight human ovarian carcinoma cell lines expressing endogenous levels of LGRs. Each curve represents inhibition of growth during a 120-hour exposure to increasing concentrations of FcF2-MMAE. Viability was determined using the CCK8 reagent.

F106R-F110R mutations in Fu_2 reduced the ratio to 2.1 ($P = 0.03$) and, when both sets of mutations were present, selectivity was abolished. Thus, in this model system, the ability to bind to both types of receptors is of substantial importance to the successful internalization of FcF2-MMAE and the liberation of free MMAE.

The effect of disabling the binding of either Fu_1 , Fu_2 , or both was further examined using the STF assay that reports

on the ability of these molecules to activate WNT signaling. As shown in Fig. 4, B and C, blocking the binding of Fu_1 to ZNRF3 and RNF43 by introducing the Q71R mutation reduced the potency of FcF2-MMAE by a factor of 24-fold ($P < 0.05$). Blocking the binding of Fu_2 to the LGR receptors reduced the IC_{50} by 87-fold; no further loss of potency occurred when both Fu_1 and Fu_2 were disabled ($P < 0.05$). These results are of greater magnitude but still consonant with those

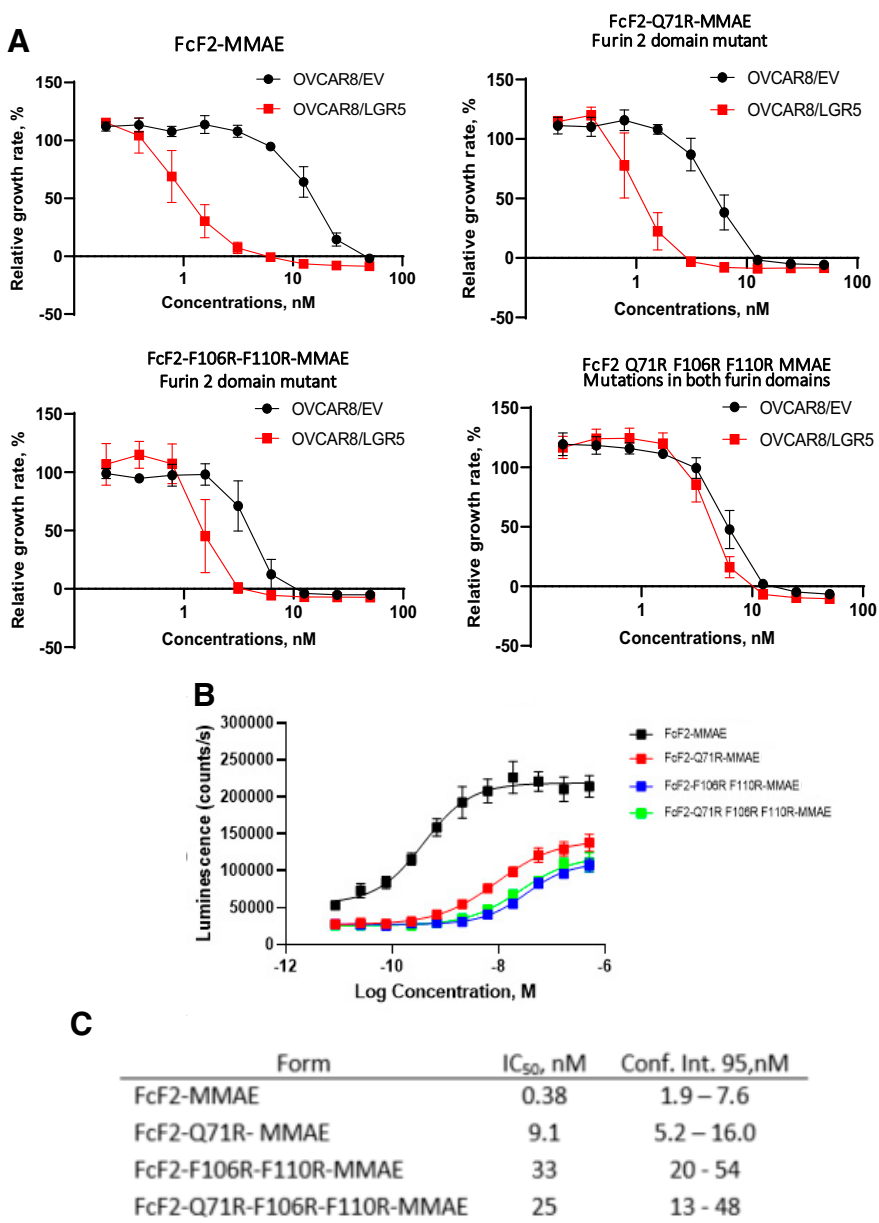


Fig. 4. Relative contribution of the Fu₁ and Fu₂ domains to the selective cytotoxicity of FcF2-MMAE. Effect of disabling the binding of either Fu₁ (FcF2-Q71R-MMAE), Fu₂ (FcF2-F106R-F110R-MMAE) or both (FcF2-Q71R-F106R-F110R-MMAE) on selectivity of growth inhibition when OVCAR8/EV and OVCAR8/LGR5 cells were exposed for 120 hours. B–C, Relative potency of FcF2-MMAE variants with respect to activation of WNT signaling in the STF assay.

Values in the table in panel C are mean ± S.E.M. IC₅₀ values from three independent STF experiments each performed with triplicate cultures.

of the cytotoxicity assay and again highlight the contribution made by both domains.

Pharmacokinetics and Pharmacodynamics of FcF2-MMAE. BALB/c mice were given a bolus intravenous injection of 0.1 nmol/g (9 μg/g) FcF2-MMAE, and plasma samples were obtained from three mice at each sampling time point. The concentration of FcF2-MMAE was measured using an ELISA with monoclonal capture and polyclonal detection antibodies of different species prepared by immunization with RSPO1 (LLQ 1.5 pmol/ml). Fig. 5A presents the composite plasma decay curve; analysis with WinNonLin curve-fitting software yielded estimates of 4.47 hours for the distribution half-life and 29.7 hours for the terminal half-life. The initial half-life was shorter than anticipated. One mechanism by which FcF2-MMAE may be removed from the plasma compartment is through binding to red blood cells, white blood

cells or platelets. However, when plasma spiked with FcF2-MMAE was added to sedimented formed elements to reconstitute their normal respective volumes, there was no significant removal of drug from the plasma fraction at 4°C over 27 hours (Supplemental Fig. 3). This suggests that the rapid initial half-life is largely due to distribution into tissues.

When administered in a large dose, RSPO1 causes a rapid but transient increase in proliferation of the gut mucosa in mice. As FcF2-MMAE contains only part of the RSPO1 molecule, we assessed its ability to engage its receptors by measuring relative potency in the STF assay. As shown in Fig. 5B, FcF2-His and FcF2-MMAE were 12.5 and 9-fold less potent than full-length RSPO1 ($P < 0.05$). However, the addition of MMAE to the FcF2-His molecule did not reduce potency, indicating that the MMAE does not distort the critical sequences in Fu₁ and Fu₂ that mediate binding.

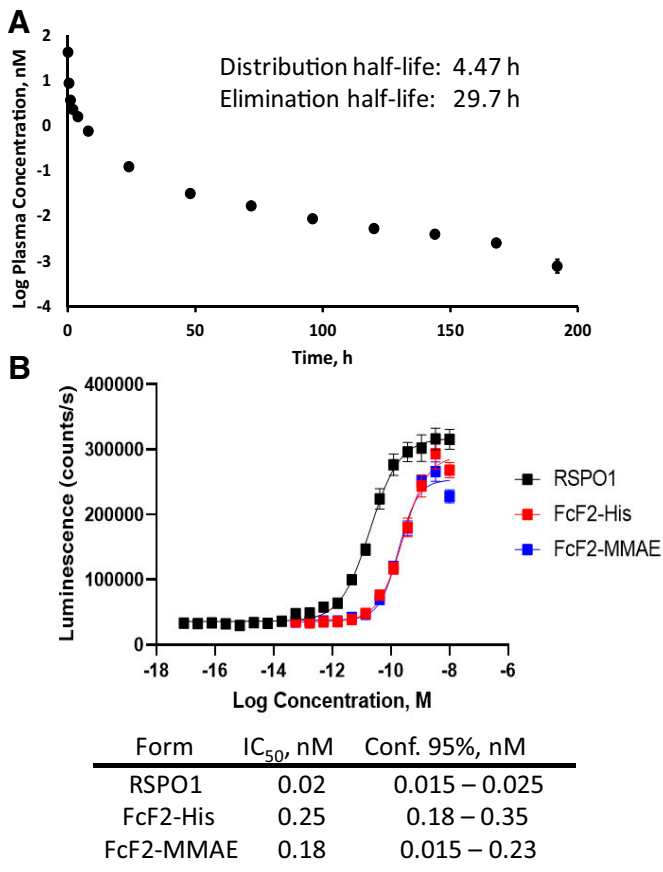


Fig. 5. Plasma pharmacokinetics and pharmacodynamics of FcF2-MMAE. A, Plasma concentration of FcF2-MMAE as a function of time following IV injection of 0.1 nmol/g (9 μ g/g) in BALB/c mice determined by ELISA. B, Relative potency of full-length RSPO1, FcF2-His and FcF2-MMAE as determined by the STF assay. Vertical bars, \pm S.E.M. of triplicate samples.

Efficacy of FcF2-MMAE in Human Ovarian Cancer Xenograft Models. Xenografts established from the isogenic pair of OVCAR8/EV and OVCAR8/LGR5 cells were used to explore both the in vivo efficacy and selectivity of FcF2-MMAE. In the experiment presented in Fig. 6A, mice were treated with 0.5 nmol/g (42.6 mg/kg) FcF2-MMAE every 4 days for four doses given by the intraperitoneal route once tumors became palpable. FcF2-MMAE had a much larger effect on the OVCAR8/LGR5 than on the OVCAR8/EV tumors. A difference in the growth rate was apparent by Day 20 and persisted to Day 61, at which point the FcF2-MMAE-treated OVCAR8/LGR5 tumors averaged only 35% of the size of the vehicle treated tumors (223 ± 58 versus 631 ± 108 , $N = 8$, $P = 0.0037$). FcF2-MMAE was also effective at slowing the growth rate of the OVCAR8/EV cells consistent with evidence that they express some combination of the LGR and/or ubiquitin ligase receptors, but the curves for the drug and vehicle-treated tumors did not separate until after 30 days and, at 60 days, the FcF2-MMAE-treated OVCAR8/EV tumors averaged 63% as large as the control tumors. It is noteworthy that, for both OVCAR8/EV and OVCAR8/LGR5 tumors, the reduction in tumor growth rate was maintained for >1.5 months after the last dose of FcF2-MMAE, an effect consistent with targeting of stem cells in the tumor from which it is difficult to recover growth rate.

Fig. 6B shows the change in average mouse weight during and after the course of four FcF2-MMAE injections at a dose of 0.5 nmol/g (42.6 mg/kg). The first injection caused a transient loss of mean body weight but it rapidly recovered and overall mice gained weight over the treatment period. There were no deaths in the animals treated with 0.5 nmol/g prior to sacrifice due to tumor burden in either the control or treatment groups. No observable adverse events, including diarrhea, change in activity level, posture or grooming or reduction in food consumption occurred after the first dose of FcF2-MMAE.

The OVCAR8/LGR5 model was used to explore the efficacy and toxicity of FcF2-MMAE as a function of dose using the more clinically relevant every 7-day schedule. The growth curves presented in Fig. 6C document an increase in efficacy as the dose was increased from 0.125 to 1.0 nmol/g. Even a dose of 0.125 nmol/g (10.6 mg/kg) produced a significant decrease in growth rate (final tumor volume 66% of untreated control). As shown in Fig. 6D, this dose produced no weight loss. Efficacy and maximal weight loss increased with dose up to 0.75 nmol/g; no further increase in either parameter was observed at 1.0 nmol/g. This experiment suggests a therapeutic window over an eight-fold dose range but FcF2-MMAE produced under GMP conditions will be required to refine this estimate.

Efficacy of FcF2-MMAE in Wild-Type Human Ovarian Cancer Xenograft Models. The efficacy of FcF2-MMAE was explored in a total of three ovarian cancer xenograft models established from cell lines that had not undergone any genetic modification to increase LGR5 and which contain very few cells that express detectable levels of LGR5. Single doses of 1.0 nmol/g (85.2 mg/kg) given intraperitoneally at the time tumors became palpable produced long delays in tumor growth in the KF-28 and CAOV3 models in the absence of dose-limiting weight loss (Fig. 7, A and B). A dose of 0.25 or 0.5 nmol/g FcF2-MMAE given on a q4dx4 (OVCAR8) or q7dx4 schedule was active against CAOV3, and KF-28 xenografts (Fig. 7, C–E) in the absence of significant toxicity in the form of weight loss (Supplemental Fig. 4). These data provide evidence for efficacy even in tumor models in which LGR5-positive cells are rare. FcF2-MMAE was effective in these three different human ovarian cancer models at low doses in the absence of molecular engineering to increase LGR5 expression. It is not currently possible to accurately define the level of expression of LGR4, LGR5, and LGR6 in these models so sensitivity cannot be linked to the expression of any one of these. However, the data are consistent with the concept that stem-like cells in each of these tumors express, in sum, enough of these receptors in their stem cell population to be responsive to FcF2-MMAE.

Discussion

The hypothesis driving interest in selectively targeting stem cells in tumors is that their destruction will limit tumor expansion and metastatic capacity. The rationale for using the receptor-binding Fu₁-Fu₂ domain of RSPO1 to achieve this goal is based on its high affinity for LGR5 and LGR6 (~3 nM) (Carmon et al., 2011) and evidence that expression of these receptors mark stem cells in tumors as they do in normal epithelia. This approach is of particular interest in the case of ovarian cancer because LGR5 and LGR6 mark stem cells in the ovarian surface and fallopian epithelia from which ovarian cancers arise (Zhang et al., 2019) and after transformation these tumors exhibit unusually high levels of expression of

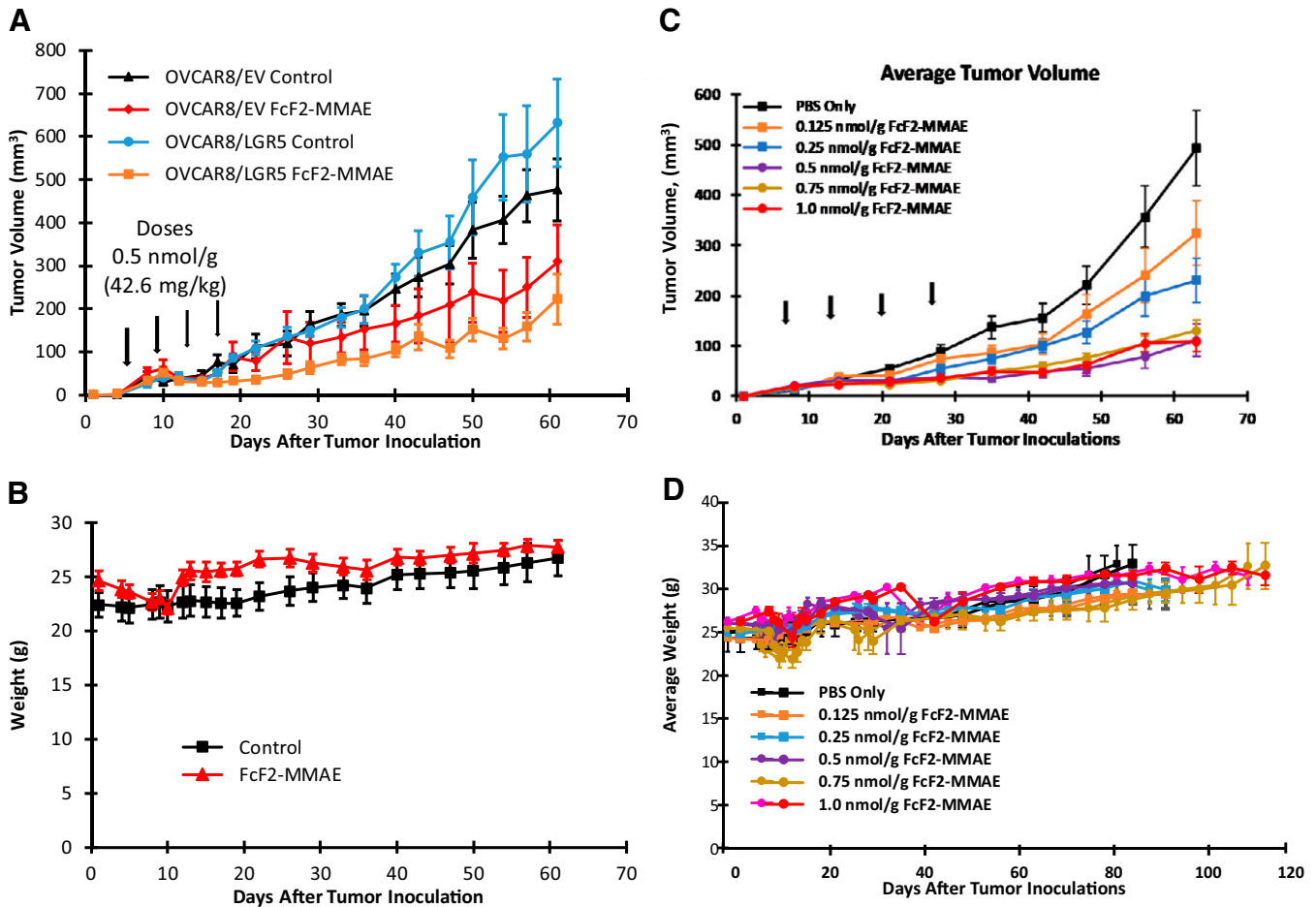


Fig. 6. Efficacy and toxicity of FcF2-MMAE against human ovarian cancer OVCAR8/EV (LGR5-low) and OVCAR8/LGR5 (LGR5-rich) xenografts. Tumor volume as a function of time (A) and mouse weight (B) during and following treatment with FcF2-MMAE 0.5 nmol/g (42.65 mg/kg) q4dx4 IP. Inhibition of OVCAR8/LGR5 growth (C) and mouse weight (D) as a function of FcF2-MMAE dose on a q7dx4 schedule. $N = 24/\text{group}$. Vertical arrows indicate dosing days. Vertical bars, \pm S.E.M.

LGR5 and LGR6 (Schindler et al., 2017; Lee et al., 2020). The fact that the Fu₁-Fu₂ domain binds in a bispecific manner to both an LGR and either ZNRF3 or RNF43 favors specificity and, as part of a normal human protein, there is a reduced risk of immunogenicity.

The development of FcF2-MMAE was informed by our prior experience with the R1FF-MMAE molecule which consisted of just the Fu₁-Fu₂ domain of RSPO1 linked to MMAE through a cleavable linker (Yu et al., 2021). Although R1FF-MMAE exhibited LGR5-dependent cytotoxicity and in vivo activity, it did not have optimal pharmaceutical properties. The modifications made to create FcF2-MMAE increased production yield, resulted in dimerization such that there were two rather than one MMAE per molecule, prolonged plasma half-life, and increased the number of Fu₁-Fu₂ receptor binding domains per molecule from one to two, potentially enhancing the avidity of binding to the LGRs and ZNRF3/RNF43 (Lee et al., 2019).

FcF2-MMAE produces LGR5-dependent killing in vitro and differentially depletes cells with the highest levels of this receptor. The mean difference of 76-fold in IC₅₀ values was sufficient to yield substantially greater in vivo efficacy against the LGR5-rich OVCAR8/LGR5 cells. The results of the cytotoxicity assays indicate that engagement with both the LGR and ubiquitin ligase receptors is important for optimum selectivity.

Given its terminal half-life of 27.4 hours, it was of interest that efficacy was better when injected every 7 rather than every 4 days. Consistent with its sub-nanomolar potency in vitro, in vivo activity was detected at a dose of just 0.125 nmol/g (10.6 mg/kg). Efficacy increased with dose up to a level approaching a maximum tolerated dose, yielding an estimate of an 8-fold therapeutic window, which is substantially higher than that of many of the chemotherapeutic agents used for the treatment of ovarian cancer. Most importantly, FcF2-MMAE demonstrated cytotoxicity at <10 nM in all but one member of a panel of ovarian cell lines and had in vivo activity in three additional ovarian xenograft models established from cells expressing only endogenous un-manipulated levels of the LGRs. Although the sum total of expression of each individual member of the LGR4-6 family cannot be accurately determined due to differing affinities of available antibodies, and of the affinity of each LGR for the RSPO1 Fu₁-Fu₂ domain in its dimeric form, this provides substantial assurance that they are high enough to allow FcF2-MMAE to be effective. LGR5 and LGR6 are expressed in the stem cells of many other types of cancer, suggesting the possibility of activity in multiple types of malignancies.

Ablation of LGR5-expressing cells in the mouse intestine does not destroy its epithelial integrity, and recent studies suggest that this is due to the plasticity of transiently amplifying cells to

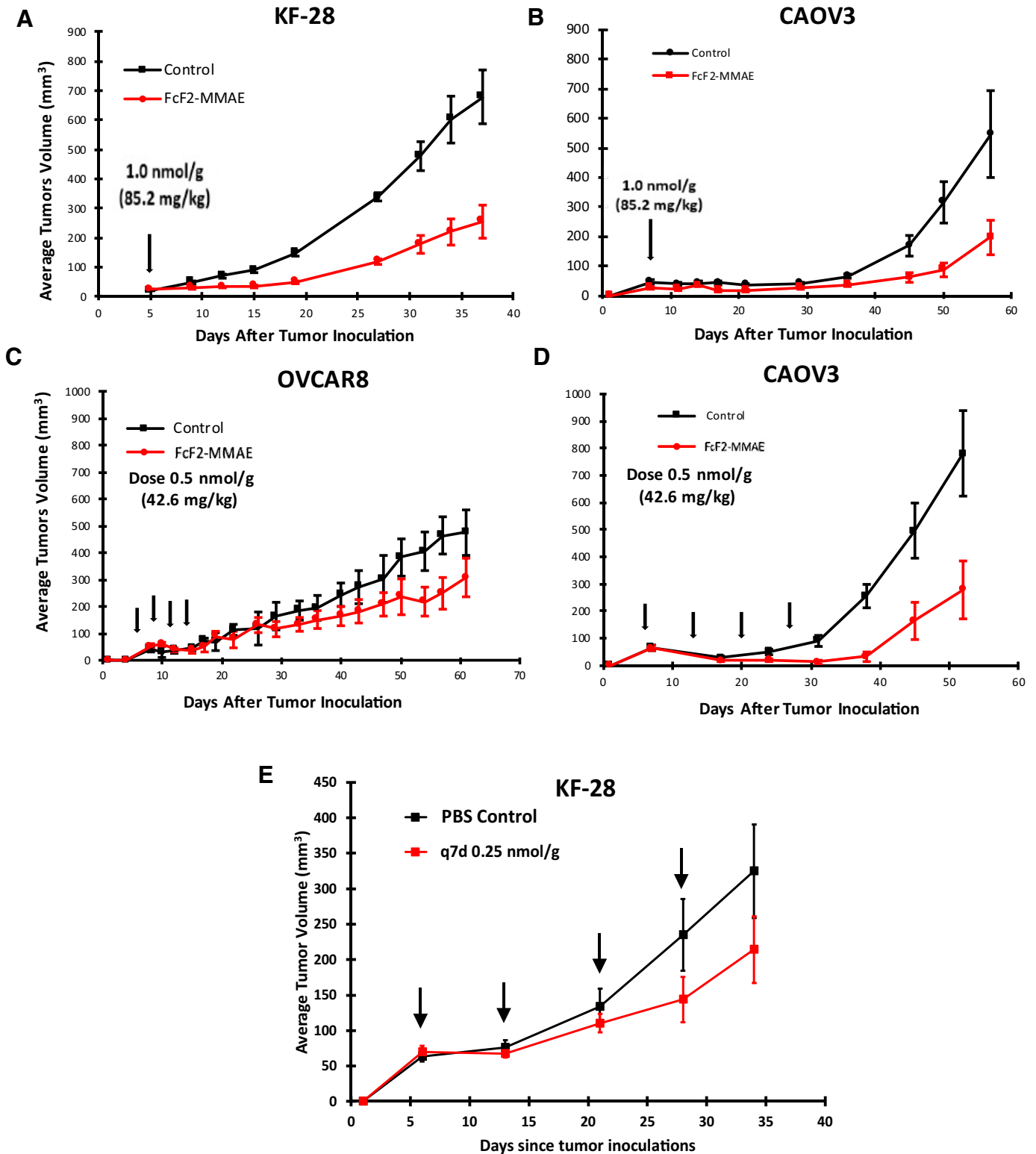


Fig. 7. Efficacy of FcF2-MMAE in wild-type ovarian cancer xenografts. Effect of a single dose of 1.0 nmol/g FcF2-MMAE on subsequent tumor growth in the KF-28 (A) and CAOV3 (B) xenograft models. C–E, Effect of multiple 0.5 nmol/g (2.6 mg/kg) doses on tumor growth in the OVCAR8 (C), CAOV3 (D), and KF-28 (E) ovarian cancer xenograft models. Vertical arrows indicate dosing days. Vertical bars, \pm S.E.M., $N = 16$ –20/group.

regenerate cells with full stem cell capabilities (Tian et al., 2011; Azkanaz et al., 2022). However, the extent to which ovarian or other types of cancer retain such plasticity remains to be defined. Studies with organoid-derived colon cancer xenografts indicate that ablation of LGR5 can produce a relatively long-lasting

response, and antibody-drug conjugates (ADCs) targeted to LGR5 produce good responses in colon cancer xenograft models (Junttila et al., 2015; Gong et al., 2016). This is consistent with the long duration of growth inhibition produced in the KF-28 and CAOV3 models by a single dose of FcF2-MMAE.

FcF2-MMAE produced unexpectedly little toxicity in mice at doses that had anti-tumor activity. The differential effect on tumors versus normal tissues is likely to be due to multiple factors beyond a possible difference in the expression of LGR5 and LGR6 by tumor stem cells versus normal stem cells. First, normal epithelia may be more tolerant to loss of LGR5-positive cells as shown for the intestine (Tian et al., 2011; Junttila et al., 2015; Gong et al., 2016). Second, in normal tissues stem cells reside in highly structured protected niches surrounded by cells that provide support in the form of WNTs, RSPO1, and cytokines. FcF2-MMAE may have much better access to tumor stem cells than stem cells in a normal epithelial niche due to differences in microanatomy and physiology. To the extent that LGRs and ZNRF3/RNF43 are expressed on the luminal rather than basal surface of stem cells when they are in a normal polarized niche, the ability of RSPO1 in plasma to access the stem cell may be limited (de Vreede et al., 2022). However, polarization is lost after transformation and FcF2-MMAE can be expected to have better access to diffusely distributed receptors on cancer stem cells once the drug arrives in the stem cell environment. Finally, FcF2-MMAE contains only the Fu₁-Fu₂ domain of RSPO1 and is missing the long C-terminal TSP-BR domain that has been shown to mediate binding to proteoglycans that favors accumulation in the niches of normal tissues (Lebensohn and Rohatgi, 2018). The missing TSP-BR domain has also been reported to limit the ability of the remaining Fu₁-Fu₂ part of the molecule to activate WNT signaling via a non-LGR-dependent pathway, a potential cause of toxicity (Dubey et al., 2020).

While FcF2-MMAE produced very few clinically observable adverse events in mice at therapeutically effective doses, there is a general concern that any drug containing the Fu₁-Fu₂ domain would drive unwanted proliferation of both normal and tumor tissues. Systemic administration of a large dose of full-length RSPO1 produces rapid but quite transient up-regulation of WNT signaling in the small intestine as detected by increases in *AXIN2* and *Ki-67* expression. A response is detectable at 3 hours, peaks at 24 hours, and has largely resolved by 48 hours (Kim et al., 2005). However, this produces no adverse clinical consequences. Repeated large daily doses produce a proliferative response in the stem cells of the jejunum (Zhou et al., 2013; Sun et al., 2021), liver (Sun et al., 2021), and skin (Weber et al., 2020), but this too is well-tolerated. Indeed, RSPO1 facilitates recovery from both radiation- and chemically-induced enteritis (Zhao et al., 2007; Zhao et al., 2009; Zhou et al., 2013). The STF analysis indicated that FcF2-MMAE is 9-fold less potent than full-length RSPO1. However, if FcF2-MMAE produces an increase in WNT signaling in vivo, the response is likely transient and not sustained when the drug is administered on a weekly schedule.

Historically it has been very difficult to develop high affinity antibodies selective for LGR5 and LGR6. Nevertheless, several investigators have explored the use of ADCs that target LGR5 to deplete stem cells in gastrointestinal tumors (Junttila et al., 2015; Gong et al., 2016; Azhdarinia et al., 2018). While good responses were observed, the magnitude of LGR5-mediated selectivity was modest. RSPO targeting has several important advantages over ADCs and, in any case, ADC development has not gone well and anti-LGR5 ADCs have not entered clinical trials. First, FcF2-MMAE uses the natural ligand which binds with nanomolar affinity and is rapidly internalized by endocytosis so that its cargo is delivered intracellularly.

Second, Fu₁-Fu₂ armed with a cytotoxin has the potential to target all three of the LGR family members (LGR4, LGR5, and LGR6) and the two ubiquitin ligase receptors ZNRF3 and RNF43 at the same time, whereas an ADC can target only a single LGR at a time. Thus, an Fu₁-Fu₂ domain armed with a cytotoxin has the potential of killing cells that have a low expression of one type of LGR or ubiquitin ligase receptor but substantial expression of another. Third, the precision with which the sortase reaction conjugates MMAE results in a more homogeneous population of molecules than is attained with conjugation to cysteines or amines. Fourth, to the extent that ZNRF3/RNF43 are also expressed on CSCs, the bispecific binding of the Fu₁-Fu₂ domain favors selectivity and an enhanced rate and extent of internalization. Fifth, there are tumors that overexpress ZNRF3 and RNF43 independently of the LGRs. Since the Fu₁ domain binds to these two receptors, it can target this type of tumor as well. Sixth, and very importantly, the Fu₁-Fu₂ domain simultaneously engages both an LGR and ZNRF3 or RNF43. In essence, this is the equivalent of a bispecific ADC; this type of ADC is currently of great interest because of their enhanced avidity, specificity, and ability to cluster receptors and mediate enhanced internalization (Shim, 2020). Overall, there is a strong rationale for the further exploration of FcF2-MMAE and of the approach of using Fu₁-Fu₂ as a targeting ligand.

Authorship Contributions

Participated in research design: Mulero, Gately, Howell.

Conducted experiments: Wong, Mulero, Barth, Wang, Shang, Tikle, Rice.

Performed data analysis: Wong, Mulero, Barth, Wang, Shang, Gately, Rice, Howell.

Wrote or contributed to the writing of the manuscript: Wong, Mulero, Howell.

References

- Azhdarinia A, Voss J, Ghosh SC, Simien JA, Hernandez Vargas S, Cui J, Yu WA, Liu Q, and Carmon KS (2018) Evaluation of Anti-LGR5 Antibodies by ImmunopET for Imaging Colorectal Tumors and Development of Antibody-Drug Conjugates. *Mol Pharm* 15:2448–2454.
- Azkanaz M, Corominas-Murtra B, Ellenbroek SIJ, Bruens L, Webb AT, Laskaris D, Oost KC, Lafrenze SJA, Annusver K, Messal HA et al. (2022) Retrograde movements determine effective stem cell numbers in the intestine. *Nature* 607:548–554.
- Barker N, Huch M, Kujala P, van de Wetering M, Snippert HJ, van Es JH, Sato T, Stange DE, Begthel H, van den Born M et al. (2010) Lgr5(+ve) stem cells drive self-renewal in the stomach and build long-lived gastric units in vitro. *Cell Stem Cell* 6:25–36.
- Carmon KS, Gong X, Lin Q, Thomas A, and Liu Q (2011) R-spondins function as ligands of the orphan receptors LGR4 and LGR5 to regulate Wnt/beta-catenin signaling. *Proc Natl Acad Sci USA* 108:11452–11457.
- Clarke MF (2019) Clinical and Therapeutic Implications of Cancer Stem Cells. *N Engl J Med* 380:2237–2245.
- Cui J, Toh Y, Park S, Yu W, Tu J, Wu L, Li L, Jacob J, Pan S, Carmon KS et al. (2021) Drug Conjugates of Antagonistic R-Spondin 4 Mutant for Simultaneous Targeting of Leucine-Rich Repeat-Containing G Protein-Coupled Receptors 4/5/6 for Cancer Treatment. *J Med Chem* 64:12572–12581.
- de Lau W, Peng WC, Gros P, and Clevers H (2014) The R-spondin/Lgr5/Rnf43 module: regulator of Wnt signal strength. *Genes Dev* 28:305–316.
- de Vreede G, Gerlach SU, and Bilder D (2022) Epithelial monitoring through ligand-receptor segregation ensures malignant cell elimination. *Science* 376:297–301.
- Dubey R, van Kerkhof P, Jordens I, Malinauskas T, Pusapati GV, McKenna JK, Li D, Carette JE, Ho M, Siebold C et al. (2020) R-spondins engage heparan sulfate proteoglycans to potentiate WNT signaling. *eLife* 9:e54469.
- Gong X, Azhdarinia A, Ghosh SC, Xiong W, An Z, Liu Q, and Carmon KS (2016) LGR5-Targeted Antibody-Drug Conjugate Eradicates Gastrointestinal Tumors and Prevents Recurrence. *Mol Cancer Ther* 15:1580–1590.
- Gupta PB, Pastushenko I, Skibinski A, Blanpain C, and Kuperwasser C (2019) Phenotypic Plasticity: Driver of Cancer Initiation, Progression, and Therapy Resistance. *Cell Stem Cell* 24:65–78.
- Hafner M, Niepel M, Chung M, and Sorger PK (2016) Growth rate inhibition metrics correct for confounders in measuring sensitivity to cancer drugs. *Nat Methods* 13:521–527.
- Junttila MR, Mao W, Wang X, Wang BE, Pham T, Flygare J, Yu SF, Yee S, Goldenberg D, Fields C et al. (2015) Targeting LGR5+ cells with an antibody-drug conjugate for the treatment of colon cancer. *Sci Transl Med* 7:314ra186.

- Kessler M, Hoffmann K, Brinkmann V, Thieck O, Jackisch S, Toelle B, Berger H, Mollenkopf HJ, Mangler M, Schouli J et al. (2015) The Notch and Wnt pathways regulate stemness and differentiation in human fallopian tube organoids. *Nat Commun* **6**:8989.
- Kim KA, Kakitani M, Zhao J, Oshima T, Tang T, Binnerts M, Liu Y, Boyle B, Park E, Emtage P et al. (2005) Mitogenic influence of human R-spondin1 on the intestinal epithelium. *Science* **309**:1256–1259.
- Lebensohn AM and Rohatgi R (2018) R-spondins can potentiate WNT signaling without LGRs. *eLife* **7**:e33126.
- Lee CH, Kang TH, Godon O, Watanabe M, Delidakis G, Gillis CM, Sterlin D, Hardy D, Cogné M, Macdonald LE et al. (2019) An engineered human Fc domain that behaves like a pH-toggle switch for ultra-long circulation persistence. *Nat Commun* **10**:5031.
- Lee S, Jun J, Kim WJ, Tamayo P, and Howell SB (2020) WNT Signaling Driven by R-spondin 1 and LGR6 in High-grade Serous Ovarian Cancer. *Anticancer Res* **40**:6017–6028.
- Peng WC, de Lau W, Madoori PK, Forneris F, Granneman JC, Clevers H, and Gros P (2013) Structures of Wnt-antagonist ZNRF3 and its complex with R-spondin 1 and implications for signaling. *PLoS One* **8**:e83110.
- Raslan AA and Yoon JK (2019) R-spondins: Multi-mode WNT signaling regulators in adult stem cells. *Int J Biochem Cell Biol* **106**:26–34.
- Sato T, Vries RG, Snippert HJ, van de Wetering M, Barker N, Stange DE, van Es JH, Abo A, Kujala P, Peters PJ et al. (2009) Single Lgr5 stem cells build crypt-villus structures in vitro without a mesenchymal niche. *Nature* **459**:262–265.
- Schindler AJ, Watanabe A, and Howell SB (2017) LGR5 and LGR6 in stem cell biology and ovarian cancer. *Oncotarget* **9**:1346–1355.
- Shim H (2020) Bispecific Antibodies and Antibody-Drug Conjugates for Cancer Therapy: Technological Considerations. *Biomolecules* **10**:360.
- Sun T, Annunziato S, Bergling S, Sheng C, Orsini V, Forcella P, Pikiolek M, Kancherla V, Holwerda S, Imanci D et al. (2021) ZNRF3 and RNF43 cooperate to safeguard metabolic liver zonation and hepatocyte proliferation. *Cell Stem Cell* **28**:1822–1837.e10.
- Tian H, Biehs B, Warming S, Leong KG, Rangell L, Klein OD, and de Sauvage FJ (2011) A reserve stem cell population in small intestine renders Lgr5-positive cells dispensable. *Nature* **478**:255–259.
- Weber EL, Lai YC, Lei M, Jiang TX, and Chuong CM (2020) Human Fetal Scalp Dermal Papilla Enriched Genes and the Role of R-Spondin-1 in the Restoration of Hair Neogenesis in Adult Mouse Cells. *Front Cell Dev Biol* **8**:583434.
- Xie Y, Zamponi R, Charlat O, Ramones M, Swalley S, Jiang X, Rivera D, Tschantz W, Lu B, Quinn L et al. (2013) Interaction with both ZNRF3 and LGR4 is required for the signalling activity of R-spondin. *EMBO Rep* **14**:1120–1126.
- Yan KS, Janda CY, Chang J, Zheng GXY, Larkin KA, Luca VC, Chia LA, Mah AT, Han A, Terry JM et al. (2017) Non-equivalence of Wnt and R-spondin ligands during Lgr5⁺ intestinal stem-cell self-renewal. *Nature* **545**:238–242.
- Yu S, Mulero MC, Chen W, Shang X, Tian S, Watanabe J, Watanabe A, Vorberg T, Wong C, Gately D et al. (2021) Therapeutic Targeting of Tumor Cells Rich in LGR Stem Cell Receptors. *Bioconjug Chem* **32**:376–384.
- Zebisch M, Xu Y, Krastev C, MacDonald BT, Chen M, Gilbert RJ, He X, and Jones EY (2013) Structural and molecular basis of ZNRF3/RNF43 transmembrane ubiquitin ligase inhibition by the Wnt agonist R-spondin. *Nat Commun* **4**:2787.
- Zhang S, Dolgalev I, Zhang T, Ran H, Levine DA, and Neel BG (2019) Both fallopian tube and ovarian surface epithelium are cells-of-origin for high-grade serous ovarian carcinoma. *Nat Commun* **10**:5367.
- Zhang Z, Broderick C, Nishimoto M, Yamaguchi T, Lee SJ, Zhang H, Chen H, Patel M, Ye J, Ponce A et al. (2020) Tissue-targeted R-spondin mimetics for liver regeneration. *Sci Rep* **10**:13951.
- Zhao J, de Vera J, Narushima S, Beck EX, Palencia S, Shinkawa P, Kim KA, Liu Y, Levy MD, Berg DJ et al. (2007) R-spondin1, a novel intestinotrophic mitogen, ameliorates experimental colitis in mice. *Gastroenterology* **132**:1331–1343.
- Zhao J, Kim KA, De Vera J, Palencia S, Wagle M, and Abo A (2009) R-Spondin1 protects mice from chemotherapy or radiation-induced oral mucositis through the canonical Wnt/beta-catenin pathway. *Proc Natl Acad Sci USA* **106**:2331–2336.
- Zhou WJ, Geng ZH, Spence JR, and Geng JG (2013) Induction of intestinal stem cells by R-spondin 1 and Slit2 augments chemoradioprotection. *Nature* **501**:107–111.

Address correspondence to: Dr. Stephen B. Howell, Moores UCSD Cancer Center, 3855 Health Sciences Drive, Mail Code 0819, La Jolla, CA 92093-0819. E-mail: showell@health.ucsd.edu
